Atmospheric Environment 113 (2015) 208–222

Contents lists available at ScienceDirect

Atmospheric Environment

journal homepage: www.elsevier.com/locate/atmosenv

Impact of a future H_2 transportation on atmospheric pollution in Europe

M.E. Popa [a, *], A.J. Segers [b], H.A.C. Denier van der Gon [b], M.C. Krol [a, c], A.J.H. Visschedijk [b], M. Schaap [b], T. Röckmann [a]

[a] Institute for Marine and Atmospheric Research Utrecht (IMAU), Utrecht University, Utrecht, Netherlands
[b] TNO, Department of Climate, Air and Sustainability, Utrecht, Netherlands
[c] Meteorology and Air Quality (MAQ), Wageningen University, Wageningen, Netherlands

HIGHLIGHTS

- European air quality improves in the future due to emission regulations.
- When road traffic is converted to H_2, air quality improves further.
- H_2 leaked into the atmosphere does not have a large negative impact on air quality.

ARTICLE INFO

Article history:
Received 1 December 2014
Received in revised form
5 March 2015
Accepted 9 March 2015
Available online 11 March 2015

Keywords:
Hydrogen vehicles
Road traffic
Air quality
Europe

ABSTRACT

Hydrogen (H_2) is being explored as a fuel for passenger vehicles; it can be used in fuel cells to power electric motors or burned in internal combustion engines. In order to evaluate the potential influence of a future H_2-based road transportation on the regional air quality in Europe, we implemented H_2 in the atmospheric transport and chemistry model LOTOS-EUROS. We simulated the present and future (2020) air quality, using emission scenarios with different proportions of H_2 vehicles and different H_2 leakage rates. The reference future scenario does not include H_2 vehicles, and assumes that all present and planned European regulations for emissions are fully implemented.

We find that, in general, the air quality in 2020 is significantly improved compared to the current situation in all scenarios, with and without H_2 cars. In the future scenario without H_2 cars, the pollution is reduced due to the strict European regulations: annually averaged CO, NO_x and PM2.5 over the model domain decrease by 15%, 30% and 20% respectively. The additional improvement brought by replacing 50% or 100% of traditionally-fueled vehicles by H_2 vehicles is smaller in absolute terms. If 50% of vehicles are using H_2, the CO, NO_x and PM2.5 decrease by 1%, 10% and 1% respectively, compared to the future scenario without H_2 cars. When all vehicles run on H_2, then additional decreases in CO, NO_x and PM2.5 are 5%, 40%, and 5% relative to the no-H_2 cars future scenario. Our study shows that H_2 vehicles may be an effective pathway to fulfill the strict future EU air quality regulations.

O_3 has a more complicated behavior – its annual average decreases in background areas, but increases in the high-NO_x area in western Europe, with the decrease in NO_x. A more detailed analysis shows that the population exposure to high O_3 levels decreases nevertheless.

In all future scenarios, traffic emissions account for only a small proportion of the total anthropogenic emissions, thus it becomes more important to better regulate emissions of non-traffic sectors.

Although atmospheric H_2 increases significantly in the high-leakage scenarios considered, the additional H_2 added into the atmosphere does not have a significant effect on the ground level air pollution in Europe.

* Corresponding author.
E-mail address: epopa2@yahoo.com (M.E. Popa).

http://dx.doi.org/10.1016/j.atmosenv.2015.03.022

1. Introduction

Road traffic is a major source of greenhouse gases and pollutants. Greenhouse gases affect the earth system globally, leading to global warming and ocean acidification. Pollution affects human health and ecosystems in particular in densely populated areas. Fine particulate matter (PM2.5) enters the lungs and enhances allergies, asthma, lung infections and long term lung diseases. PM2.5 is recognized as one of the main pollutants reducing life expectancy in Europe (EEA, 2013); recent studies show that PM2.5 affects health already at levels much lower than present European air quality limits (Beelen et al., 2014). NO_x contributes to acid rain formation; it is a precursor for tropospheric ozone, aerosols and other toxic chemicals, and affects human health, especially the respiratory system (EEA, 2013; WHO, 2013). CO is a precursor for tropospheric ozone, participates in atmospheric chemistry, and is a toxic gas, affecting blood ability to transport oxygen. Tropospheric O_3 is not emitted directly but formed under influence of NO_x and volatile organic compound (VOC) emissions. It is one of the major components of photochemical smog; it affects human health, ecosystems and causes important crop losses (EEA, 2013; WHO, 2006, 2008).

In Europe (EU 28), emissions from road traffic were responsible for about 25% of the total CO emissions, 39% of NO_x and 15% of the primary PM2.5 in 2012 (EEA, 2014). Road transport was responsible for 26% of O_3 precursor emissions in Europe in 2007 (EEA, 2010).

Replacing fossil fuels by H_2 in a potential future "hydrogen economy" is attractive, in the context of reducing availability of fossil fuels and increased awareness on the problems of pollution and climate change. When using fuel cell technology, H_2 burning emits only water, thus using H_2 as a fuel would avoid direct emissions of both anthropogenic greenhouse gases and pollutants.

Regarding H_2 safety, it is often thought that H_2 would be a dangerous fuel quickly leading to explosions. However, with adequate handling, H_2 can be a safer fuel than e.g. gasoline or methanol: because of its high buoyancy it does not accumulate around leak points, reducing the risk of explosions; also, a H_2 fire causes fewer toxic emissions and less severe radiant heat damage (Adamson and Pearson, 2000; Veziroglu and Barbir, 1992).

However, it is important to consider all potential effects. In 2000s, several studies (Prather, 2003; Schultz et al., 2003; Tromp et al., 2003; Warwick et al., 2004) drew attention to the fact that a hydrogen economy would be associated with an increase in atmospheric H_2 due to leakage, and this additional atmospheric H_2 could have negative effects on the atmosphere. Additional H_2 in the atmosphere could enhance the stratospheric ozone hole (Tromp et al., 2003), and could indirectly increase the radiative forcing by influencing the greenhouse gases methane and tropospheric ozone (Prather, 2003). Later, more detailed studies showed that these negative effects are much smaller than feared initially, and small compared to the potential benefits (Derwent et al., 2006; Jacobson, 2008; Vogel et al., 2012; Wang et al., 2013b; Warwick et al., 2004).

The benefits of a hydrogen economy can be significant, especially regarding air quality. All studies to date reported considerable improvements in air quality, if (part of) the economy or transportation were switched to H_2 as an energy carrier. The first studies on this subject considered the present (~2000) situation and assumed an immediate transition to a H_2 economy.

In their modeling study, Schultz et al. (2003) considered a conversion to H_2 of 50% of the total economy (which is roughly equivalent to 100% conversion of the transportation sector). This resulted in decreases in simulated NO_x (30%), CO (3%) and O_3 (5%) mole fractions. They also found that in polluted areas in Western Europe, China and Eastern US the average surface O_3 would increase; however, even in these areas, the peak O_3 values were predicted to decrease, which would result in fewer violations of air quality limits. Another finding of this study was a decrease in oxidizing power of the troposphere, because the decrease in NO_x leads to less OH.

In a similar study, Warwick et al. (2004) assumed a complete replacement of the fossil fuel economy, and found reductions in tropospheric O_3 (2.2%) and OH (5%).

Jacobson et al. (2005) assumed a conversion of all US vehicles to H_2, and compared the effects on air quality, health and climate for several H_2 production options. Unlike the other studies, they also took into account the emissions associated to the production of H_2. The results showed that using H_2 produced from wind energy offers the largest benefits for health and climate. For all H_2 production methods, significant reductions were found for CO, O_3, NO_x, black carbon, and other tropospheric pollutants.

Jacobson (2008) estimated the effects of converting the global vehicle fleet to H_2 produced by wind-powered electrolysis, and found reductions over 10 years in tropospheric CO (5%), NO_x (5–13%), O_3 (6%) and OH (4%).

The recent study of Wang et al. (2013a), which estimated the effects of converting the global transportation to H_2, is the first one to place the simulations in the future (2050). The study is global, and includes higher resolution simulations with focus on the US territory. Their baseline (no H_2 cars) emission scenarios are based on the Intergovernmental Panel on Climate Change (IPCC) Special Report on Emission Scenarios (SRES) growth scenarios A1F1 and B1 (Nakicenovic et al., 2000), combined with present-day fossil fuel burning emission factors. A1F1 and B1 are the highest and lowest emission SRES scenarios. Both assume a large population increases and a world integrated economically; the A1F1 scenario assumes rapid economic growth and intensive use of fossil fuels, while in B1 the economy becomes more information oriented and less material intensive, and employs more clean and resource efficient technologies. The simulations using these baseline scenarios predict significantly increased air pollution in 2050 compared to present. The pollution decreases then significantly compared to the baseline when switching all the road traffic to H_2. The largest improvements are found in most polluted, highly populated areas. Wang et al. assume no emissions of air pollutants are associated with H_2 production.

In the present study we investigate the effects on air quality in Europe of a future (2020) H_2 -based road transportation sector, using the chemistry transport model LOTOS-EUROS. We compare future emission scenarios in which 50% or 100% vehicles are converted to H_2, with a future "baseline" scenario without H_2 vehicles. Our baseline emission scenario assumes that the current and planned European legislation concerning emissions of air pollutants is fully implemented. We account for NO_x emissions associated to the production of H_2 for vehicle use.

2. Methods

2.1. Model

LOTOS-EUROS is an Eulerian 3D chemistry transport model designed to simulate air pollution in the lower troposphere in Europe (Schaap et al., 2008). The model has been used to simulate for example ozone (Vautard et al., 2006; Schaap et al., 2008), particulate matter (Manders et al., 2009), secondary inorganic aerosol (Schaap et al., 2004a; Erisman and Schaap, 2004), black carbon

(Schaap et al., 2004b; Schaap and Denier van der Gon, 2007) and sea salt (Manders et al., 2010). LOTOS-EUROS is also being used to provide daily forecasts of air pollution over Europe and the Netherlands.

Concerning the European forecasts, LOTOS-EUROS is one of the 7 CTMs that together form the MACC regional air quality ensemble (http://gmes-atmosphere.eu/), and its performance in simulating current concentration levels is therefore continuously verified against surface observations and the other models (Marécal et al., 2015). In addition, the model has been included in dedicated validation and model inter-comparison studies (Solazzo et al., 2013; Kukkonen et al., 2012; Vautard et al., 2012). During all these verifications and comparisons, LOTOS-EUROS was found to have a performance comparable to other European regional models. Similarly to other models, LOTOS-EUROS underestimates the concentration of particulate matter (PM) due to unknown sources and missing secondary organic aerosols, and the simulated ozone variability is too low (underestimation of high values and overestimation of low values, also a common feature of models).

In the current study, the LOTOS-EUROS domain is between 35°N and 70°N latitude and between 10°W and 40°E longitude, with a spatial resolution of 0.50° lon × 0.25° lat. The vertical structure is relatively simple, with four vertical levels (surface, mixed layer and two reservoir layers) up to a height of 3500 m a.s.l. The surface layer height is fixed at 25 m; the height of the mixed layer is provided by ECMWF meteorology (see below) and the two reservoir layers are equal in height and calculated from the difference between 3500 m and the mixed layer height, with a minimum of 500 m.

For this work we use LOTOS-EUROS version 1.9.6 with ECMWF meteorological fields for 2008. The temporal resolution of the model output is 1 h. Initial and boundary conditions are provided by daily output at 6° × 4° spatial resolution from the global model TM5 (Krol et al., 2005; Pieterse et al., 2011, 2013).

Gas phase chemistry is computed in LOTOS-EUROS using the CBM-IV scheme (Whitten et al., 1980), with updates as described in Schaap et al. (2008). Aerosol chemistry is represented using the ISORROPIA2 thermodynamic equilibrium module (Fountoukis and Nenes, 2007). Dry deposition of gases is implemented through the module DEPAC 3.11 (Van Zanten et al., 2010) and relies on the parallel resistance approach. The deposition velocity of CO was set in this work equal to half of the H_2 deposition velocity (see below). The dry deposition of particles follows the parameterization of Zhang et al. (2001). Below cloud scavenging is described using simple scavenging coefficients for gases (Schaap et al., 2004a) and particles (Simpson et al., 2003).

2.2. Present emissions

The anthropogenic emissions (for CH_4, CO, NH_3, VOC, NO_x, SO_x, PM10, PM2.5, CO_2) are derived from the TNO-MACC emission grids (Kuenen et al., 2014). The emissions include both grid and point sources and are aggregated into 10 main source categories (SNAP ("Selected Nomenclature for Sources of Air Pollution"), level 1), with the road traffic category separated into 5 sub-categories.

Anthropogenic emissions vary with month, day of week, and time of day according to time factors per source category (Mues et al., 2014). Emissions of VOCs and CO from road traffic vary additionally with atmospheric temperature (Sauter et al., 2012).

2.3. Implementation of H_2 in LOTOS-EUROS

We added into the CBM-IV chemistry scheme used in LOTOS-EUROS the production of H_2 by formaldehyde photolysis (CH_2O ($h\nu$) → CO + H_2) and the reaction of H_2 with OH ($H_2 + OH + O_2 \rightarrow HO_2 + H_2O$). Through the second reaction, H_2 can directly influence the atmospheric composition and chemistry, due to destruction of OH and production of HO_2. For this reaction we use the temperature dependent reaction rate as given in Houweling et al. (1998) based on DeMore et al. (1994).

The TNO MACC emission data were modified to include H_2 from stationary and mobile fossil fuel combustion. Combustion of traditional fossil fuels emits H_2, and these H_2 emissions are usually well correlated with CO emissions. Emissions of H_2 from fossil fuel road traffic were computed based on the emissions rates per vehicle category available in literature (Bond et al., 2011 and references therein). For the categories for which no emission rates were available (most of the pre-Euro 3 vehicles), H_2 emissions were computed by scaling the CO emissions with a factor of 0.55 mol:mol (Bond et al., 2011; Vollmer et al., 2007). Only gasoline and gas-fueled vehicles are assumed to emit relevant amounts of H_2; Diesel vehicles emit negligible amounts of H_2 (Bond et al., 2010, 2011). The temperature dependence of H_2 emissions from road traffic was set equal to the one of CO. Besides the H_2 emissions from fossil fuel burning, in the future scenarios that include H_2 cars, additional emissions of H_2 due to H_2 fuel leakage were added, as described in Section 2.4.

The anthropogenic H_2 emissions from other combustion sources were computed by scaling the CO emissions with a factor of 0.4 mol:mol, which is approximately in the middle of the range estimated from atmospheric measurements (Hammer et al., 2009; Yver et al., 2009, 2011).

Soil uptake is the main sink for atmospheric H_2, accounting for about 80% of the atmospheric H_2 loss. Soil uptake of H_2 is computed in LOTOS-EUROS by multiplying the deposition velocity with the local mole fraction. The deposition velocity depends on land use and on soil conditions, with lower deposition velocity for wet or frozen soil. No significant H_2 deposition takes place over water bodies and onto plants. Note that, due to its atmospheric lifetime of about 2 years, the H_2 abundance in the LOTOS-EUROS domain is largely determined by the applied boundary conditions from TM5.

2.4. Emission scenarios

In order to assess the potential impact of a future change to H_2 powered vehicles, six main emission scenarios were created as summarized in Table 1. The "NOW" scenario represents the present situation and uses emissions for the year 2005. The other scenarios represent the future (2020) and include no H_2 cars (CLE2020), 50% H_2 cars (H2_50_01 and H2_50_4), or 100% H_2 cars (H2_100_01 and H2_100_4). The "_01" and "_4" codes in the scenario names refer to the 0.1% and 4% H_2 leakage rates (see below). The CLE2020 ("Current Legislation") scenario assumes that all current and planned European emission regulations will be fully implemented by 2020. We considered the H_2 vehicles are fuel cell − powered, therefore they do not emit NO_x.

Table 1
Emission scenarios.

Scenario	Time	H_2 vehicles	H_2 leak rate
NOW	Present	0	0
CLE2020	Future	0	0
H2_50_01	Future	50%	0.1%
H2_50_4	Future	50%	4%
H2_100_01	Future	100%	0.1%
H2_100_4	Future	100%	4%

We considered large proportions of H_2 powered vehicles, in order to be able to detect even small effects. It is obviously highly unlikely that a large proportion of vehicles (e.g. 50%) will be using H_2 by the year 2020. The reason we chose the year 2020 for our simulations, and not for example 2050, is that the human population distribution, energy demands, the road traffic location and intensity, and other relevant variables can to some extent be predicted for 2020 but not much further into the future.

For the future scenarios that include H_2 vehicles, we used two H_2 leak rate scenarios of 0.1% and 4% that define what we consider a possible range. Although H_2 is difficult to confine, and higher leak rates (10% or more) have been predicted by some authors (e.g. Tromp et al., 2003), we assume that for financial reasons the losses will be limited to a lower level of 4% in a mature technology. Our high leak rate (4%) is consistent to the estimates of Bond et al., 2011. The 0.1% leak rate is very optimistic, but it is considered achievable by some authors, as it is already attainable in some of the present-day technical systems – e.g., the H_2 distribution grid in Germany (Bond et al., 2011; Lovins, 2003; Zittel and Altmann, 1996).

In our scenarios, H_2 for vehicle use is produced by steam reforming of natural gas coupled with carbon capture and storage (Damen et al., 2006; Spath and Mann, 2000), at natural gas-fired power plant locations. The only emission from H_2 production is NO_x, at an approximate rate of 0.01 kg NO_x/kg H_2 (rate based on system total NO_x emission from Spath and Mann, 2000). The required amount of H_2 for transportation is calculated based on an efficiency increase of 25% when switching from conventional fuels to H_2, plus the amount of H_2 needed to compensate for leakage losses. Note that H_2 also has approximately a factor three higher energy content on a mass basis than conventional fuels.

The TM5 boundary conditions (see Section 2.1) are identical for all present and future simulations, which means that future possible changes in the background levels of H_2 or other species are not considered.

3. Results

3.1. Emissions

Fig. 1 shows the annual anthropogenic emissions of CO, NMVOC, NO_x, PM2.5 and H_2, over the whole model domain, for each of the six scenarios. It is evident that, at present, the road traffic contribution to the total emissions is substantial. For the CLE2020 scenario, the emissions of all species decrease significantly compared to present, due to decreases in both traffic and non-traffic categories of emissions; the traffic contribution to the total emissions decreases as well. For the scenarios that assume 50% H_2 cars (H2_50_01 and H2_50_4) the total emissions for all species except H_2 are slightly lower than for CLE2020, and the emissions decrease further for the scenarios with 100% H_2 cars (H2_100_01 and H2_100_4). The difference between the 100% H_2 cars scenarios and 50% scenarios is larger than the difference between the 50% H_2 cars scenarios and CLE2020. That is because the first 50% H_2 cars are assumed to be bought instead of new, low pollution traditional fuel cars, therefore they replace the cleaner half of the CLE2020 fleet; the second 50% H_2 cars replace all the rest of the cars, including the older, more polluting ones. The non-traffic NO_x emissions increase slightly in the H_2-vehicle scenarios, due to the addition of NO_x emissions during H_2 production.

The emissions of H_2 decrease in the CLE2020 scenario compared to the present, due to fewer emissions from fossil fuel burning. For the H_2-vehicle scenarios with low leakage rate (H2_50_01 and H2_100_01) the total H_2 emissions are slightly higher than in CLE2020, but still lower than the present emissions. For the scenarios with high leakage rates (H2_50_4 and H2_100_4), H_2 emissions increase significantly.

3.2. The present atmosphere (NOW scenario)

Fig. 2 shows annual mean ground level concentrations of H_2, CO, PM2.5, NO_x, O_3 and OH for the NOW and CLE2020 simulations, and the relative differences between the two scenarios. The results corresponding to the present atmosphere are in the leftmost panels.

Within Europe, the area including Benelux, Germany, part of the UK and part of central Europe is the most polluted, because of its high population density, industry and dense road network. High mole fractions of CO and NO_x are due to large emissions, mainly from road traffic.

Regarding O_3, this high NO_x area is in the VOC limited regime, in which O_3 decreases with the increase in NO_x due to the titration effect (O_3 reacts with the emitted NO, converting it to NO_2, e.g. Sillman, 1999); the result is a decrease of the average O_3 below the regional background level.

OH is also depleted in this area due to less production from O_3 and the sink of OH through the OH + NO_2 reaction. In the

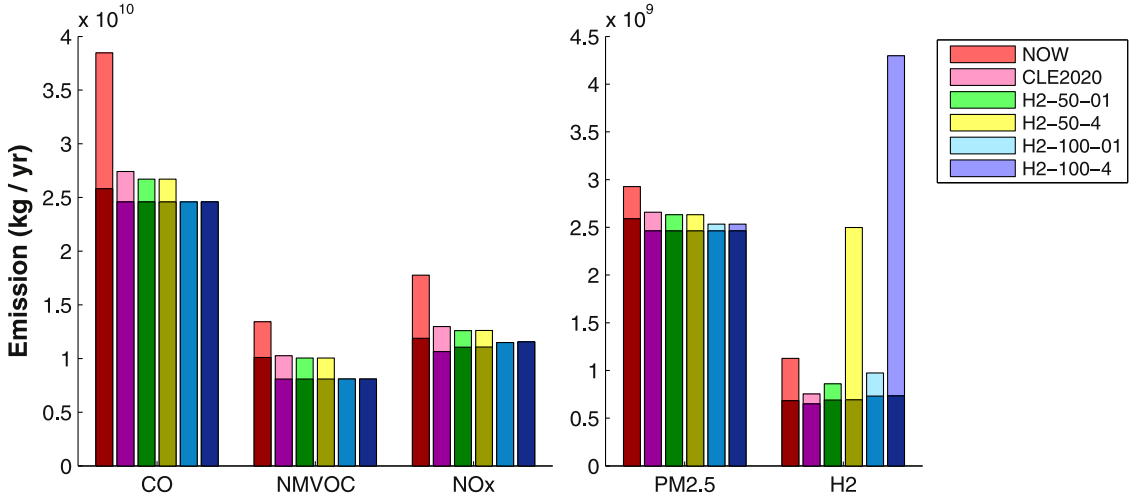

Fig. 1. Total annual emissions in the model domain for different scenarios. The upper, light-colored bar portions represent the contribution of road traffic emissions. (For interpretation of the references to colour in this figure legend, the reader is referred to the web version of this article.).

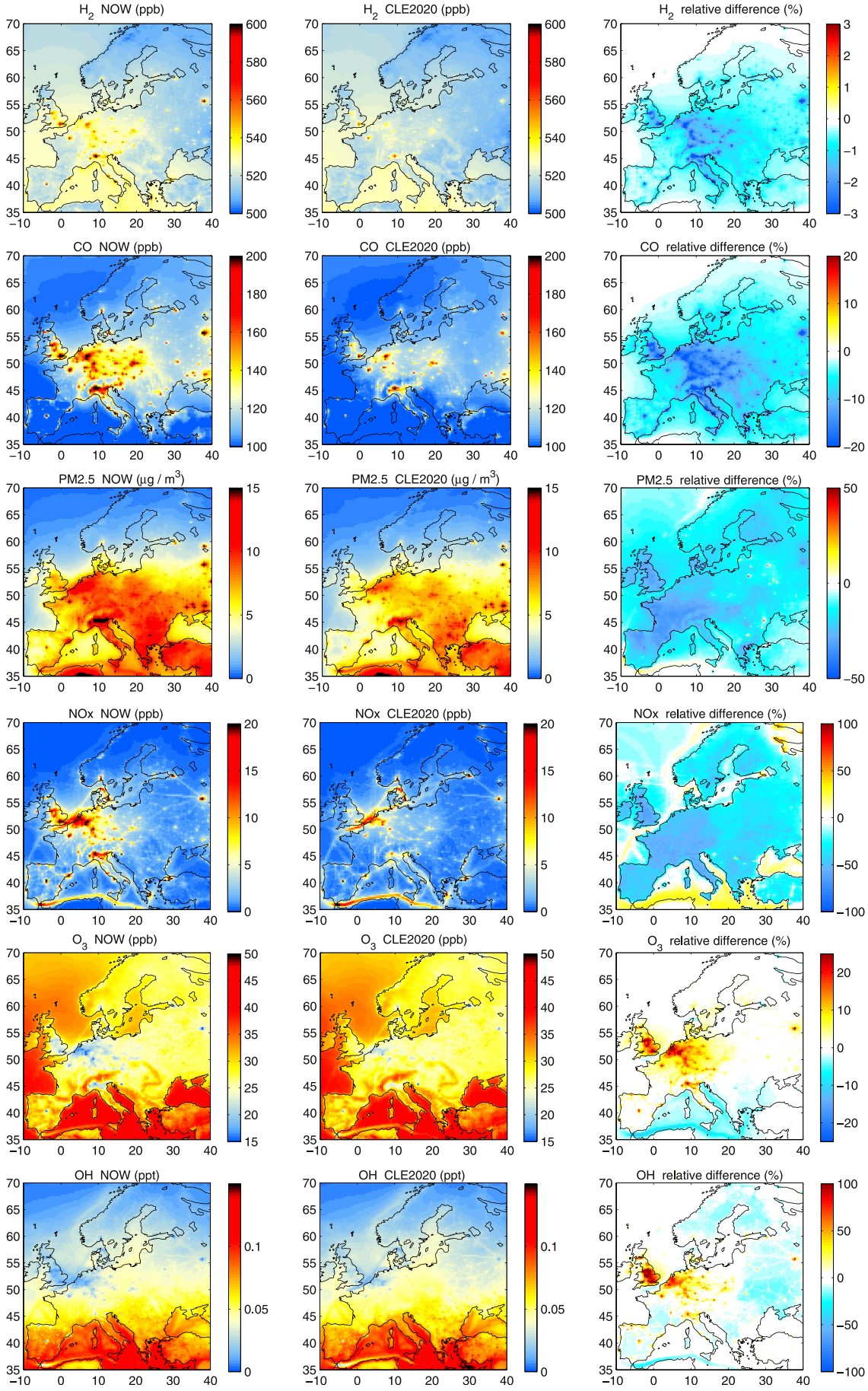

Fig. 2. H_2, CO, PM2.5, NO_x, O_3 and OH over Europe for the NOW and CLE2020 scenarios, and the relative differences between the two scenarios for each species. The figure shows annual means at ground level. Note that the color scales are different. (For interpretation of the references to colour in this figure legend, the reader is referred to the web version of this article.).

eastern part of the model domain, high CO is largely due to power production. H_2 is also higher in polluted areas, because it is emitted together with CO from anthropogenic burning processes. PM2.5 has a more uniform distribution over the land areas south of 55°N, with several high concentration areas (around 20 μg/m^3) in northern Italy and urbanized areas in south-east Europe.

3.3. The future without H_2 cars (CLE2020 − NOW)

As shown in Section 3.1, the emissions decrease in the CLE2020 scenario compared to present; it is thus predictable that the air quality improves accordingly. Indeed, it is evident in Fig. 2 that CO, PM2.5 and NO_x mole fractions decrease in the CLE2020 scenario relative to the present.

In the CLE2020 simulation, the spatial distribution of CO is similar to NOW, but the mole fractions decrease significantly. The decrease in CO is largest over high CO areas, both in absolute and in relative terms. The average decrease in CO in our domain is 15 ppb (15%). In polluted areas CO decreases by up to 30 ppb (25%). H_2 mole fractions also decrease, due to the decrease in emissions, similarly to CO. The average H_2 decrease is 3 ppb (0.5%), with lager decreases of up to 30 ppb in polluted areas.

PM2.5 decreases uniformly in western Europe by approximately 2 μg/m^3 (20%). In central and eastern Europe the general decrease is smaller, and there are several urban centers in central Europe where a slight increase can be observed, but the PM 2.5 level still remains below 10 μg/m^3. In northern Italy the average PM 2.5 decreased to less than 15 μg/m^3.

NO_x decreases significantly in all land areas. The relative decrease is of roughly 50% in western Europe and 30% in eastern Europe; the absolute decrease is largest in polluted areas. NO_x increases however over the ship tracks in Mediterranean by up to 3 ppb (20%), due to the fact that ship emissions are less regulated. Even if emissions and atmospheric mole fractions of NO_x decreased, there are still areas with average NO_x above 10 ppb, in particular Benelux, and the average NO_x can reach more than 20 ppb around urban centers.

O_3 behaves unlike the other pollutants: it generally increases over the most polluted areas, by up to 5 ppb or 25%. These are the areas where at present the O_3 is decreased below the continental background level, due to high NO_x. The decrease in NO_x in the CLE2020 scenario leads to an increase in O_3 towards the background level. In the southern part of Europe, the background O_3 decreases slightly (by up to 5%), and the decrease is larger along the ship tracks. This decrease is the result of the increased NO_x in those areas. The behavior of O_3 for all scenarios is analyzed in more detail in Section 3.5.

OH decreases by about 10% over the “clean” land areas, due to the combined opposite effects of less production from O_3 and less consumption by NO_x and CO. OH also decreases over the ship tracks in the Mediterranean; here the reason is an increased OH sink due to the increase in NO_x from ships. Over land, in the most polluted regions, where the decrease in NO_x is largest, OH increases in the CLE2020 scenario because of the decrease in consumption by reaction with NO_x, and increased production from enhanced O_3.

3.4. The future with H_2 cars

In this section we compare the simulations including 50% and 100% H_2 cars with the CLE2020 results. We use for this comparison the low leak rate scenarios, H2_50_01 and H2_100_01 (the low and

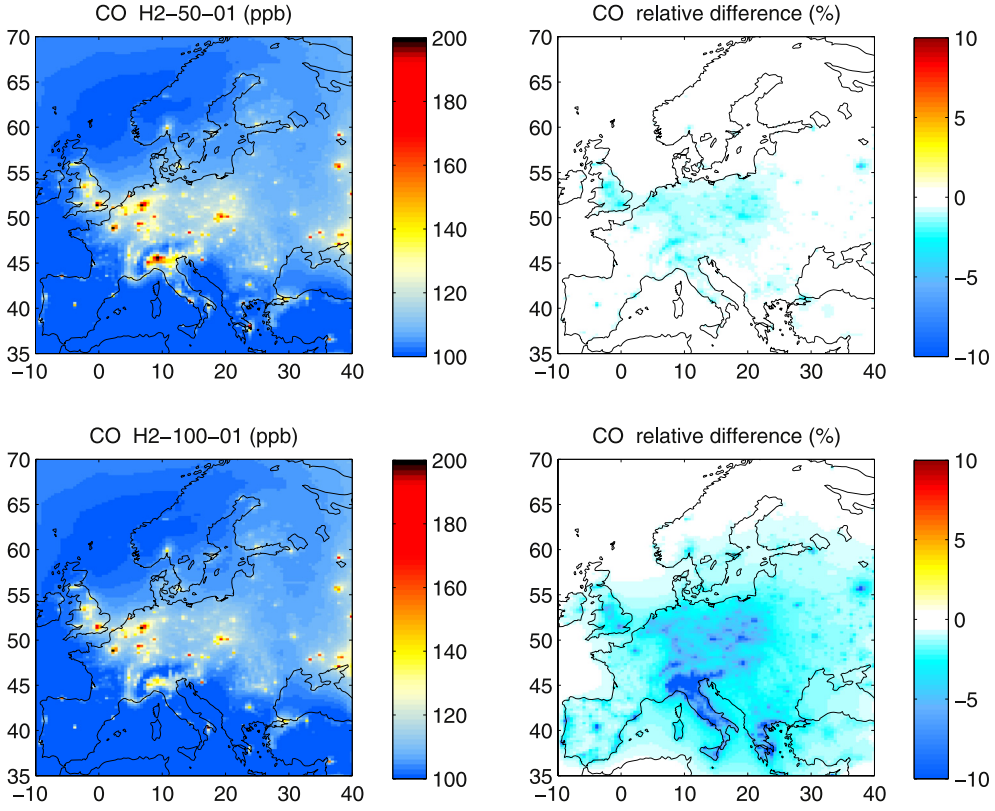

Fig. 3. CO mole fractions for the simulations with 50% (H2_50_01) and 100% (H2_100_01) H_2 cars (left panels), and the relative differences between these and the CLE2020 simulation (right panels). The figure shows annual means at ground level. Note that the color scales are different between left and right panels. (For interpretation of the references to colour in this figure legend, the reader is referred to the web version of this article.).

high leak rate scenarios will be compared in Section 3.6). Each species is discussed in detail below, except for H_2 which is discussed in Section 3.6.

Fig. 3 shows the annual average CO mole fractions at ground level for the H2_50_01 and H2_100_01 scenarios (50% and 100% H_2 cars), and the relative differences to the CLE2020 scenario. For the H2_50_01 scenario, CO slightly decreases compared to CLE2020, by up to 2–3 ppb in western and central Europe. The decrease is small because, as already mentioned in Section 3.1, the relatively clean cars are the first to be replaced by H_2 cars (that is, a new and clean car in the CLE2020 scenario corresponds to a H_2-car in the H2_50_01, while the dirty old cars remain on the road in both scenarios). The decrease in the H2_100_01 scenario (100% H_2 cars) is larger, of up to 10 ppb (~10%) in western and central Europe. The largest decrease of approximately 20 ppb occurs in northern Italy, due to the replacement of traditional fuel with H_2 in two-wheelers.

PM 2.5, like CO, decreases very little in the H2_50_01 scenario compared to the CLE2020 (Fig. 4). The decrease is less than 1%, and is quite uniform over the land areas. For the H2_100_01 scenario, the decrease is larger, of up to 1 μg/m^3, or 10%. In western Europe, the largest decrease is in northern Italy. This scenario also results in a significant decrease in PM 2.5 in eastern Europe, of 5–10% and locally larger in some urban areas.

In the scenario with 50% H_2 cars (Fig. 5) the average NO_x decreases by 0.5 ppb in medium polluted areas and by up to 2 ppb in most polluted urban areas; the relative decrease over western Europe is of 10–15%. In the scenario with 100% H_2 cars, the NO_x decreases even more. The relative decrease over western and southern Europe and urban areas in eastern Europe is of 30–50 %; the absolute decrease is up to 3 ppb in polluted areas and up to 5 ppb in most polluted urban centers. In this scenario, only few cities in Europe still have average NO_x mole fractions of more than 10 ppb. The highest NO_x regions are now over sea, along the ship tracks in Mediterranean, English Channel and the North Sea. Transported emissions from ships become in this case one of the significant sources of pollution in the coastal areas in Benelux and UK.

Average ground O_3 is shown in Fig. 6 for the H2_50_01 and H2_100_01 scenarios, together with the differences between these and the CLE2020 scenario. Converting 50% of cars to H_2 cars in the H2_50_01 scenario has a small influence on O_3 (compared to CLE2020): background O_3 in south and south-east Europe decreases by 0.2–0.3 %, while in polluted areas it increases by up to 4%. For the H2_100_01 scenario the changes are larger: background O_3 decreases by 1–2%, while in polluted areas O_3 increases by up to 10%. These changes are qualitatively similar to the ones between the CLE2020 and NOW scenarios: in polluted areas, where NO_x decreased the most, O_3 increases towards the continental background due to less chemical consumption; in background areas O_3 decreases due to less precursor emissions. In absolute values, the O_3 never increases in polluted areas above the continental background. This relative increase in O_3 in western European polluted regions is a well-known feature, and it has been shown that decreasing precursor emissions does not always lead to a decrease in O_3 population exposure in urban areas (e.g. Colette et al., 2011). The behavior of O_3 for all scenarios is analyzed in more detail in Section 3.5.

OH (Fig. 7) has a behavior similar to the one of O_3. In the polluted areas in western Europe, the OH mole fraction recovers towards the regional background (increased production from O_3, and decreased consumption by NO_x and CO); the largest changes,

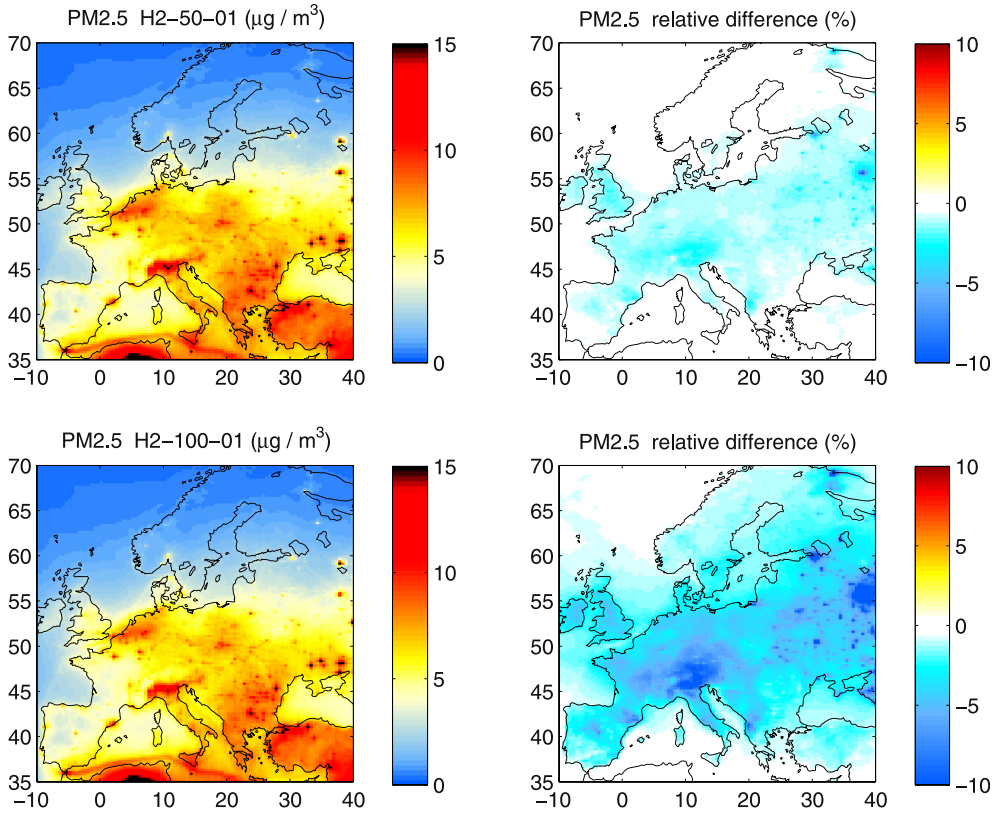

Fig. 4. PM 2.5 concentrations for the simulations with 50% (H2_50_01) and 100% (H2_100_01) H_2 cars (left panels), and the relative differences between these and the CLE2020 simulation (right panels). The figure shows annual means at ground level. Note that the color scales are different between left and right panels. (For interpretation of the references to colour in this figure legend, the reader is referred to the web version of this article.).

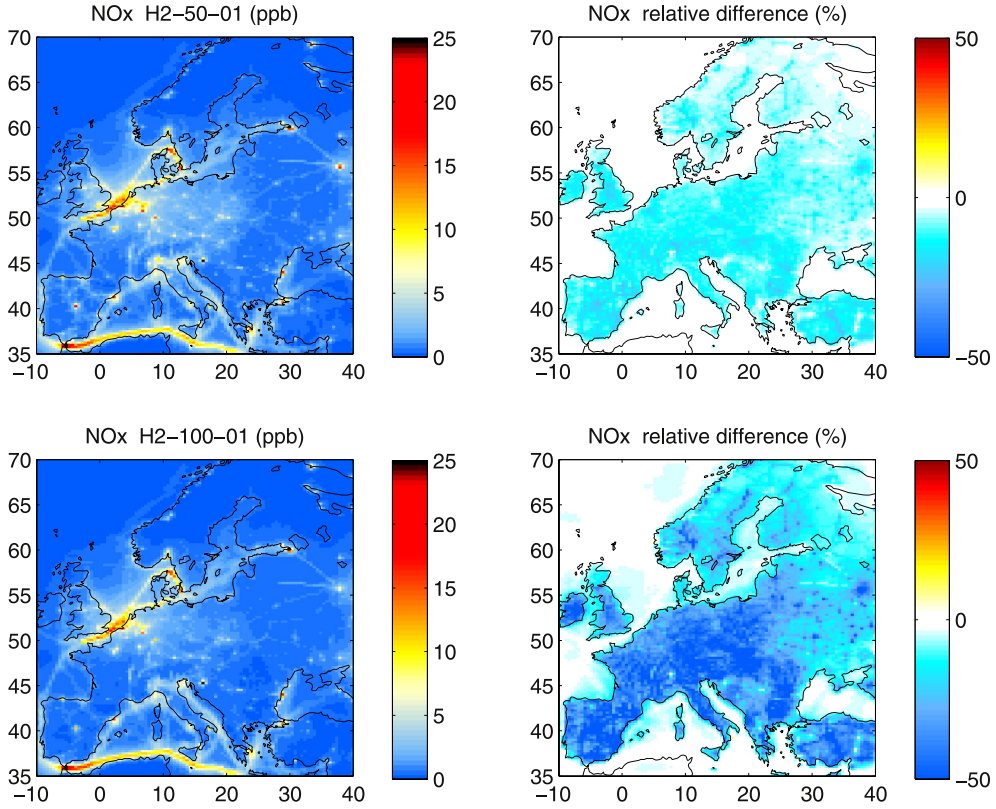

Fig. 5. NO_x mole fractions for the simulations with 50% (H2_50_01) and 100% (H2_100_01) H_2 cars (left panels), and the relative difference between these and the CLE2020 simulation (right panels). The figure shows annual means at ground level. Note that the color scales are different between left and right panels. (For interpretation of the references to colour in this figure legend, the reader is referred to the web version of this article.).

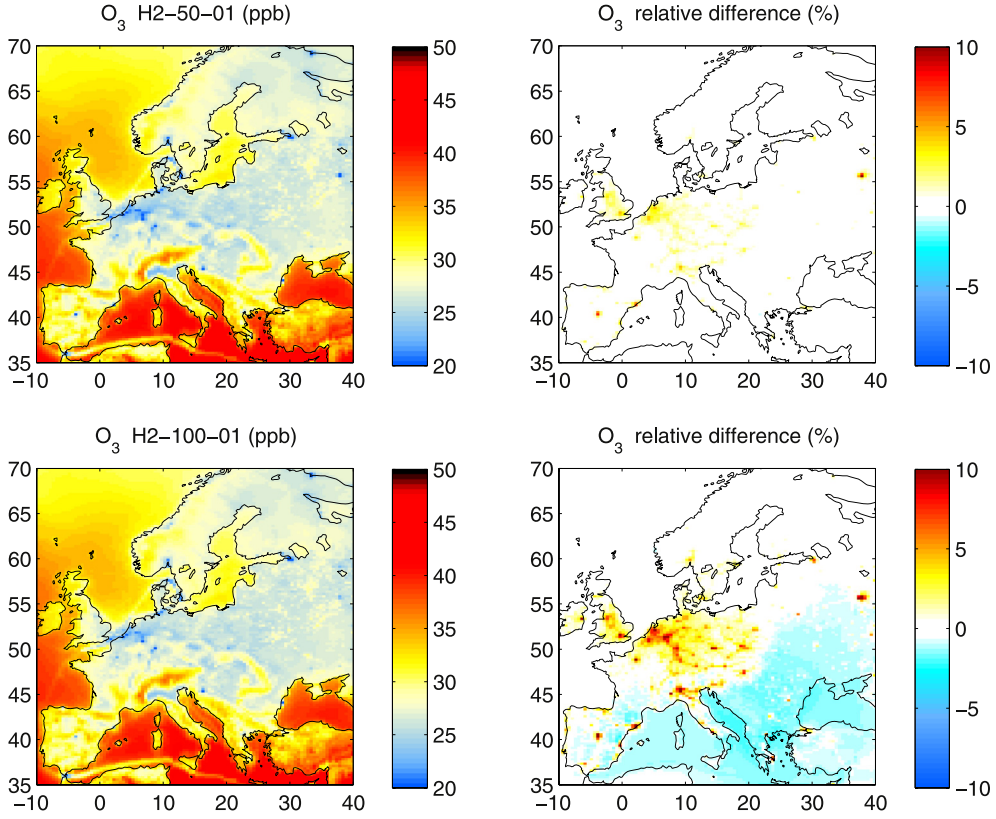

Fig. 6. O_3 mole fractions for the simulations with 50% (H2_50_01) and 100% (H2_100_01) H_2 cars (left panels), and the relative difference between these and the CLE2020 simulation (right panels). The figure shows annual means at ground level. Note that the color scales are different between left and right panels. (For interpretation of the references to colour in this figure legend, the reader is referred to the web version of this article.).

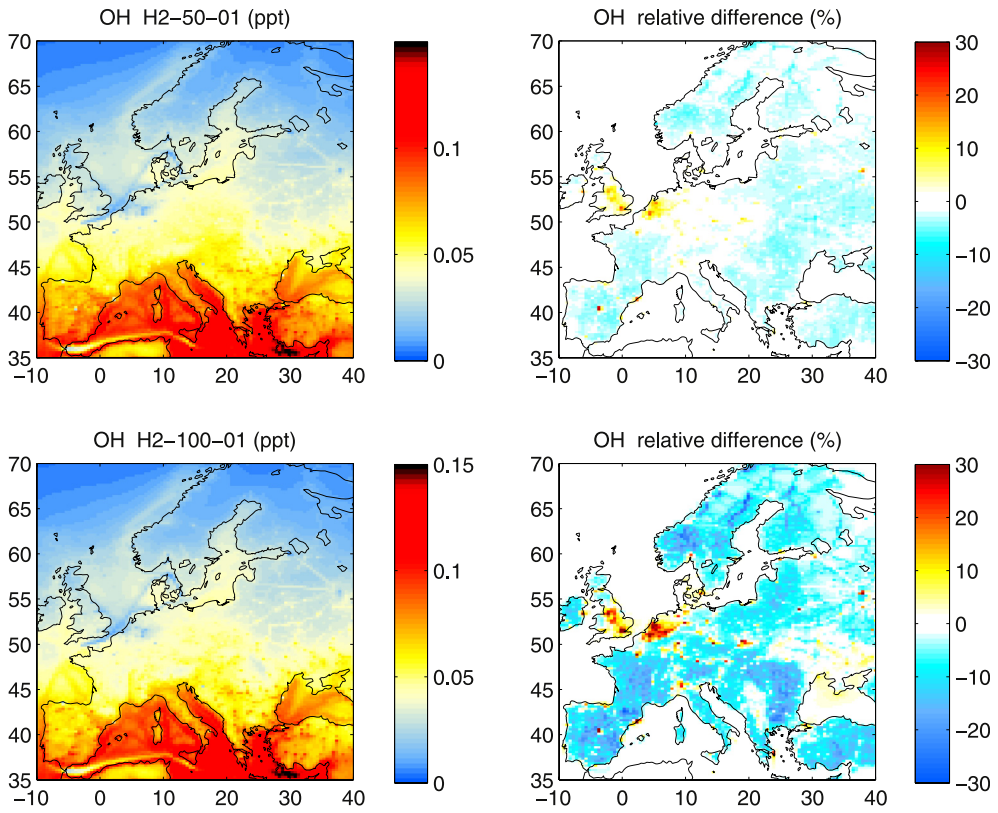

Fig. 7. OH mole fractions for the simulations with 50% (H2_50_01) and 100% (H2_100_01) H_2 cars (left panels), and the relative difference between these and the CLE2020 simulation (right panels). The figure shows annual means at ground level. Note that the color scales are different between left and right panels. (For interpretation of the references to colour in this figure legend, the reader is referred to the web version of this article.).

of up to 10% in the H2_50_01 scenario and 30% in the H2_100_01 scenario, are in Benelux and the UK. The background OH decreases over land areas by up to 5% in H2_50_01 and up to 20% in H2_100_01. This decrease is the net effect of decreased production from O_3 and decreased consumption by NO_x and CO. The absolute OH decrease is much larger in southern than in northern Europe.

3.5. O_3 detailed analysis

As already shown, O_3 behaves differently than the other pollutants, because of the complex chemistry controlling its mole fractions. In our simulations, the annual average of O_3 over the whole model domain did not change significantly in the future scenarios compared to present. However, when looking at smaller spatial scale, there are patterns that may seem contradictory: in polluted areas (e.g. Benelux and UK) the O_3 increased for the future (cleaner) scenarios, while the background O_3 decreased slightly.

O_3 mole fractions are highly variable in time, being higher during day than during night, and higher in summer than in winter. The damaging effects on human health and ecosystem are mainly related to the high summer day-time mole fractions. Fig. 8 shows the average diurnal variation in O_3 for the whole year, and the summer and winter months separately; the separate panels show averages over the whole model domain, and over the polluted area of Benelux, separately. Although the whole-domain, whole-year diurnal cycle does not change between the scenarios, in the summer diurnal cycle a small decrease for the future scenarios (compared to the present) is evident; this decrease is largest during the day-time maximum. When looking separately at the Benelux area (where the annual average O_3 increased significantly for the future scenarios), we see that the increase is larger during night time and during winter, thus when the mole fractions are lowest. That means that the O_3 maxima increase less than the mean mole fractions. Also, it is evident from this figure that the O_3 maxima in the polluted areas (where the O_3 annual average increased) are still well below the background.

Fig. 9 shows the proportion of the population in our model domain that is exposed to different levels of O_3. Plot 9a shows the scaled person hours (that is, scaled to the total number of persons in our domain and to the total number of hours in our simulation) for each level of O_3, for each scenario, calculated over 1 year using hourly data; plot 9b shows, for the same data, the differences between the future scenarios and the present. The O_3 values (x-axis) were binned in 2-ppb intervals. We used population count distribution for the year 1995 based on the Gridded Population of the World, Version 2 (GPWv2, 2000). This figure shows that the exposure of the population to medium levels of O_3 (approx. 20–45 ppb) increases in the future scenarios, while the exposure to high levels of O_3 (>45 ppb) decreases; the exposure to very low levels of O_3 decreases as well. Also, there are significant differences between the future scenarios – the decrease in exposure to high levels of O_3 (and the increase in exposure to medium O_3) is larger for the H_2-vehicle scenarios. The picture is qualitatively similar when looking separately at the Benelux area (Fig S1 in the Supplementary material). For this area, however, the increase in exposure to medium levels of O_3 is larger, while the decrease in exposure to high levels of O_3 is much smaller than over the whole model domain.

We made a similar comparison for the 8-hr running mean daily maxima of O_3 calculated following the procedure used for assessing population exposure (EU, 2008). The results are presented in the

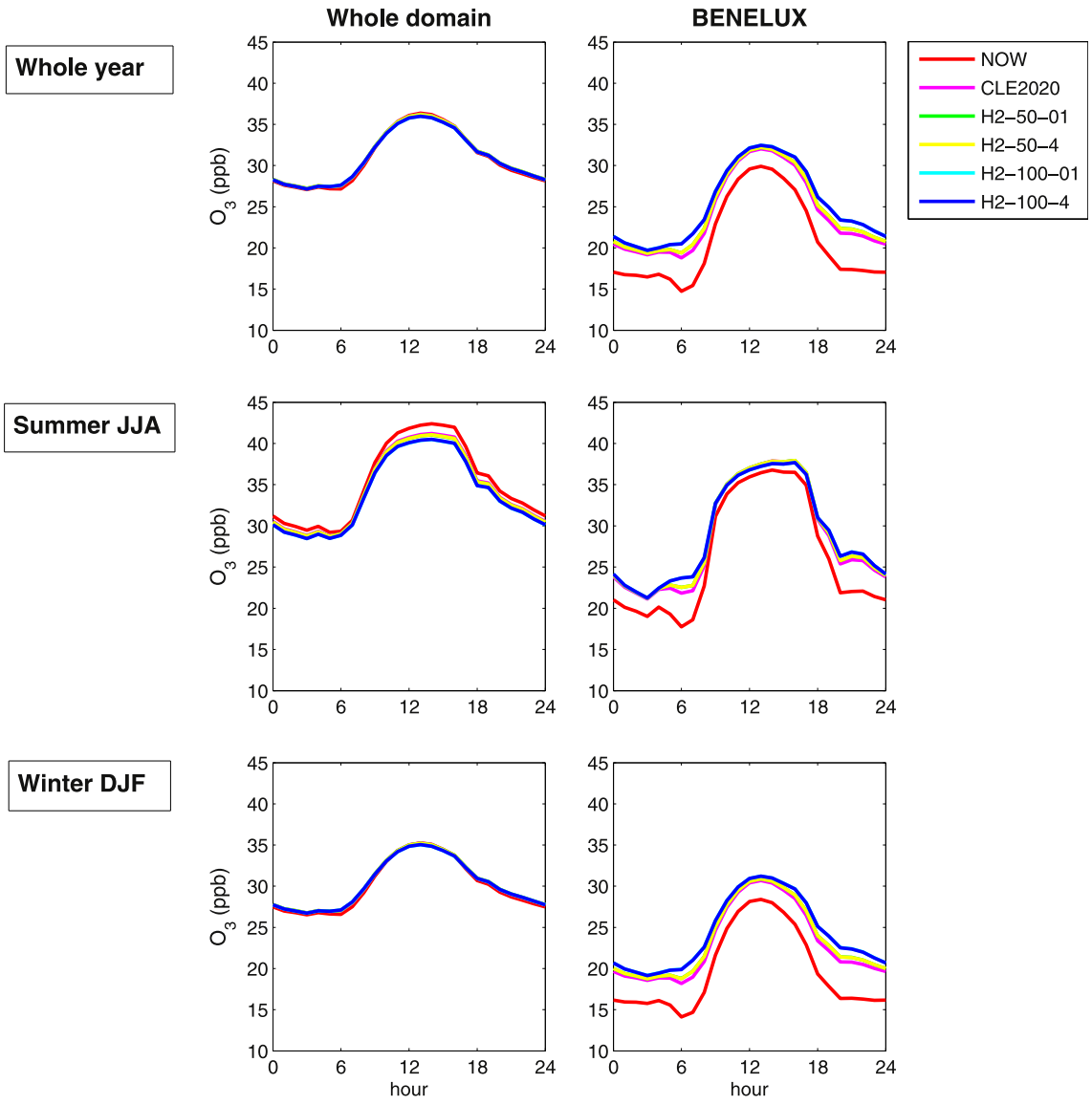

Fig. 8. Average diurnal cycles of O_3, from top to bottom: whole year, summer (Jun–Aug), and winter (Dec–Feb). The left plots show diurnal cycles over the whole LE domain. For the middle and right plots, two highly polluted regions in western Europe were selected, one in Benelux (lon 4 … 10 °W, lat 50 … 52.5 °N) and one in UK (lon −3 … 1 °W, lat 51 … 54 °N).

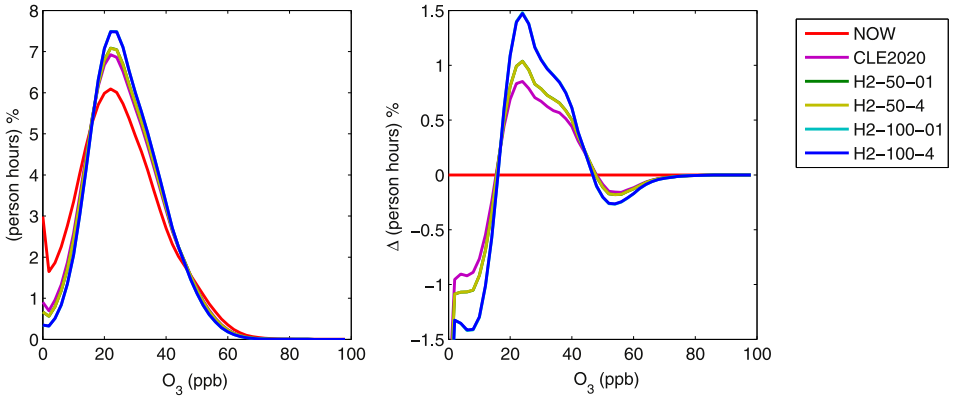

Fig. 9. Population exposed to different levels of O_3 for the different scenarios, for the whole LOTOS-EUROS domain. (left) Person hours versus O_3 level for the whole year, scaled by the total population in the domain and the total number of hours, and expressed in %. (right) Differences in person hours (%) between each scenario and the NOW scenario. Note that the y-values depend on the O_3 bin size; the O_3 bins used here are 2 ppb.

Supplementary material, for the whole model domain, and separately for Benelux area (Fig. S2). The general picture for the whole domain is similar to the one based on 1-hr data: the number of person days exposed to high (>45 ppb) O_3 8-hr maxima decreases, while the exposure to medium levels of O_3 increases. The number of person days that exceed the European and WHO limits (60 ppb (EU, 2008), and 50 ppb (WHO, 2006), respectively) is lower in the future scenarios compared to the present, and again lower in the H_2-vehicle scenarios compared to CLE2020. Although the tendency is similar for the polluted Benelux area, the decrease in population exposure to high levels of O_3 is very small here, while the increase in the population exposure to medium levels of O_3 is relatively large. Note, however, that the overall O_3 mole fractions are smaller in this area than for the whole model domain average, and there are much fewer occurrences of daily maximum 8-hr averages above 60 ppb to begin with.

In summary, the observed increases in the annual average O_3 for the future scenarios mainly arise from increases during low O_3 levels; the overall population exposure to high O_3 levels, both in terms of hourly averages and of daily maximum 8-hr means, decreases significantly (over the whole domain) or does not change much (in Benelux); and the population exposure to medium level O_3 increases.

3.6. Influence of the H_2 leak rate

In this section we compare the scenarios with low H_2 leak rate (0.1% H_2 leak, scenarios H2_50_01 and H2_100_01) with the scenarios with high H_2 leak rate (4% H_2 leak, scenarios H2_50_4 and H2_100_4) for estimating the influence of the additional H_2 emissions on the atmospheric composition.

Fig. 10 shows the relative differences in annual average ground level H_2 between the four scenarios including H_2 cars and the CLE2020 scenario. The atmospheric mole fraction of H_2 increases in all scenarios including H_2 cars, relative to the CLE2020 scenario. In the low leakage scenarios, however, anthropogenic emissions of H_2 are lower than today (NOW), and atmospheric levels of H_2 are slightly lower than today as well (not shown in figure). In the high leakage scenarios, ground level atmospheric H_2 averaged over the model domain increases by approx. 5% in H2_50_4 and 10% in H2_100_4 compared to CLE2020. The increase is largest in high road density areas; here the H_2 can increase locally by up to 20% in H2_50_4 and by 50% in H2_100_4. It should be noted that, as H_2 is a long lived species and in our simulation the lateral and top boundaries are fixed, this result is likely an underestimation of the potential increase in atmospheric H_2 over Europe.

For the 100% H_2 cars scenarios, the difference between 4% and 0.1% H_2 leak rates leads to a decrease in OH of up to 1% (Fig. 11). The associated increase in NO_x is of up to 1% and the effect on the other species is much smaller. There is no noticeable effect on CH_4 – which is expected, since CH_4 has a lifetime of 9 years, and its residence time within our domain is only several days. Thus, the H_2 added into the atmosphere can lead to small increases in some pollutants (e.g. NO_x), but the effect is much smaller that the decrease in pollution due to the decrease in pollutant and precursor emissions in H_2 scenarios compared to CLE2020. Note that this estimate only refers to the influence of H_2 on other species within our limited domain; the global influences cannot be assessed from our study.

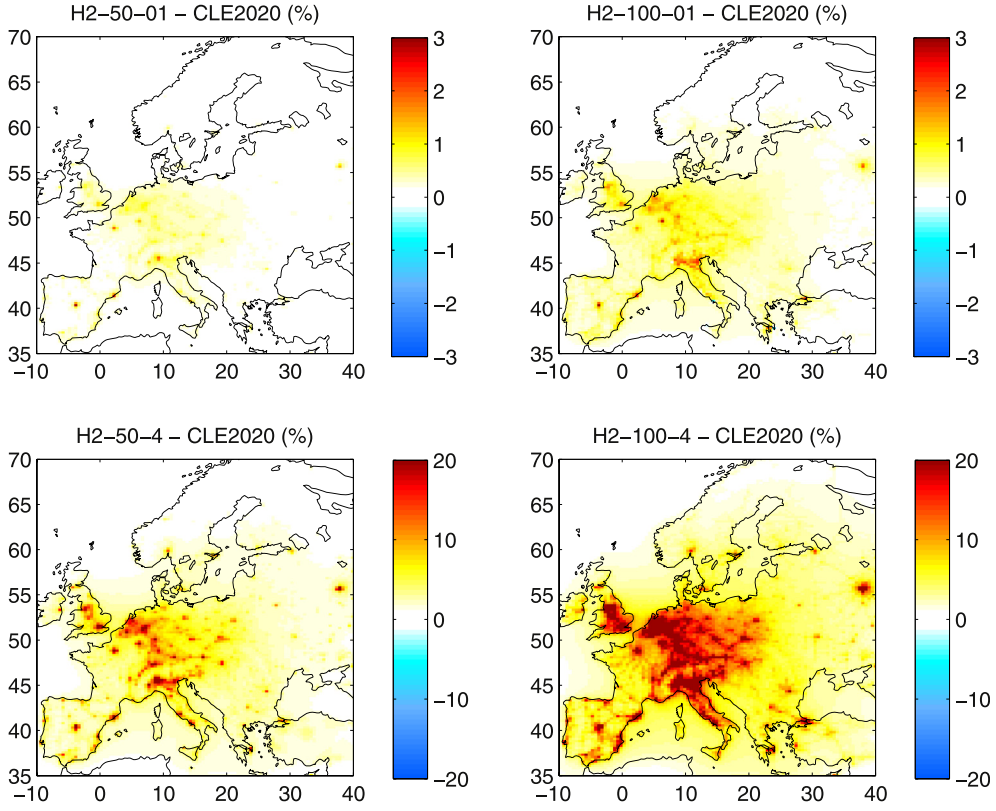

Fig. 10. Relative differences in H_2 mole fractions between the scenarios including H_2 cars (H2_50_01, H2_50_4, H2_100_01 and H2_100_4) and the CLE2020 scenario. The plots show annual averages of ground level mole fractions. Note the difference between color scales. (For interpretation of the references to colour in this figure legend, the reader is referred to the web version of this article.).

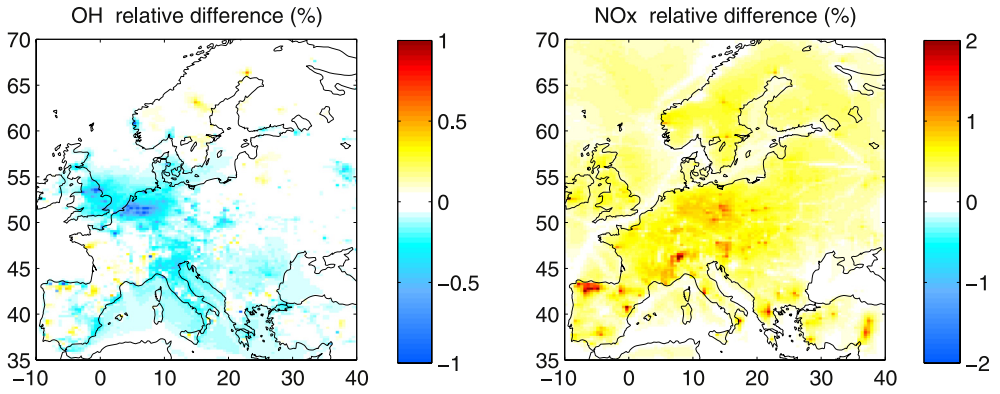

Fig. 11. Influence of the H_2 leak rate on OH and NO_x. The figure shows the relative differences between the high and low leak scenarios H2_100_4 and H2_100_01.

4. Discussion and conclusions

We simulated the future air quality in Europe, replacing part of or all traditionally-fuelled vehicles by H_2 vehicles (fuel cell), and taking into account the present and planned European legislation.

In general, our simulations show that the air quality will improve in the future in the CLE2020 scenario, and further (smaller) improvements will occur if land transportation will be converted to H_2. As expected, the largest improvements in air quality occur in and around urban centers, where the influence on human health is large.

One important aspect of our study is that in our reference scenario (CLE2020), the future atmosphere is much cleaner than the present one, even without H_2 cars. This is because Europe has current and planned regulations much stricter than most of the world, and we assume these will be all successfully implemented. Because of this already clean future atmosphere, the additional improvement brought by the H_2 vehicles is relatively small. This is the major difference between our work and the previous studies on the effect on air quality of a H_2-based economy (Jacobson, 2008; Jacobson et al., 2005; Schultz et al., 2003; Wang et al., 2013a; Warwick et al., 2004). All these previous works compared a highly polluted "baseline" situation with a clean H_2 scenario, and found dramatic improvements in air quality when (part of) the economy or transportation is converted to H_2.

Our study is the second after Wang et al. (2013a) to place the simulations in the future. Wang et al. performed global simulations, with a higher resolution focus area over the US territory. Their baseline emission scenarios are based on the IPCC-SRES growth scenarios A1F1 and B1 (Nakicenovic et al., 2000), combined with present-day fossil fuel burning emission factors. The simulations using these baseline scenarios predict significantly increased air pollution in 2050 compared to present, which is in contrast to our baseline being the relatively clean CLE2020 scenario. Therefore, in their simulation, the air quality then improves significantly, compared to the highly polluted future baseline, when switching all the road traffic to H_2.

The differences discussed above reflect the much stricter European traffic emission regulations, both present and future, compared to the rest of the world. However, these are based on existing and planned regulations, and not on existing technology. In practice, complying with stricter emission limits becomes gradually more difficult from a technological point of view. Our results show that H_2 vehicles could be, in fact, part of the solution to fulfill the future European low emission requirements.

Among all pollutants considered, particulate matter has the largest effects on human health. There is a clear quantitative relationship between PM exposure and increased mortality and morbidity, and no threshold has been identified below which no damage to health is observed (e.g. Hoek et al., 2013; Pope et al., 2002; WHO, 2006). In Europe, outdoor exposure to fine PM leads to about 100 000 deaths and 725 000 years of life lost annually (WHO, 2002). Assuming a linear relationship between the PM2.5 levels and mortality, the decrease in PM2.5 of about 20% between the NOW and CLE2020 simulations (Section 3.3) would lead to a decrease of 20% in the PM2.5 related mortality, thus to about 20 000 deaths avoided annually in Europe.

While most pollutants decrease with the decrease in emissions, ground level O_3 behaves differently, due to the complex atmospheric chemistry controlling its mole fractions. At present, a high NO_x region exists in western Europe, roughly covering Benelux and the south-eastern part of the UK, where O_3 is on average lower than the continental background, due to titration by NO. Here, O_3 production is in the VOC limited regime, and increases with the decrease in NO_x emissions, as seen in our future simulations. The annual average O_3 increases in this region in the future scenarios; the increase in O_3 in this region is however largest under low-O_3 conditions (night and winter). Despite this increase in average O_3 mole fractions, the population exposure to very high day-time ozone mole fraction decreases over the entirety of Europe. Nevertheless, the O_3 situation in Benelux highlights the importance of controlling VOC emissions, in particular in this area.

In the present scenario (NOW), traffic emissions account for an important fraction of total emissions. In the CLE2020 scenario (without H_2 cars), traffic emissions decrease significantly, and much more than the emissions from other categories; the consequence is that traffic emissions become a much smaller contributor to the total. As shown in this paper, H_2 cars still reduce emissions and atmospheric mole fractions further. However, the other emission categories become proportionally more important and, for further improvements in air quality, stricter regulations on emissions from non-road traffic sectors (e.g. sea traffic) are necessary, and possibly more effective.

For example, while for most categories the emissions decrease in the future, shipping emissions increase in all future scenarios compared to the present, and their relative contribution to pollution increases even more as road traffic emissions decrease. That is because shipping emission regulations are currently quite lenient. The pollution from ships is also transported towards coastal regions and affects densely populated regions in Benelux and UK. This is thus an issue that still needs and can be improved by setting stricter emission regulations.

One other important result of this work is related to the additional H_2 released into the atmosphere through leakage. Although

the reaction of this additional H_2 with OH leads to small increases in several pollutants, the effect is small compared to the decrease in pollutants that comes with the decreases in pollutant emissions. Because of this, the results of our study can be considered as representative for the effect on air quality of any other low emission technology. The high leakage scenarios lead however to considerable increases in atmospheric H_2; moreover, this increase is likely underestimated in our simulations because of fixed lateral and top boundaries. The increased atmospheric H_2 can have effects on the global atmosphere that cannot be estimated with our modeling setup.

The main sources of uncertainty in our results are due to (1) model errors and (2) uncertainties in emissions. Uncertainties in model simulations could arise from lack or insufficient parameterization of physical processes, finite resolutions, limited input data, etc. The model performance is therefore continuously verified by comparison with observations (Section 2.1). Note that the impact of model uncertainties is limited by focusing on yearly average concentrations as the end-result: while hourly concentrations can differ substantial from observations, the yearly average is much more accurate. However, since we use the same model setup and meteorology for all the simulations, the uncertainties of the relative differences reported are mainly driven by the uncertainties in emissions. For O_3 and NO_x, additional uncertainties are related to the ability of the model to simulate the nonlinear chemistry of these species, and are difficult to estimate. The emission data include uncertainties in activity data (5–10% for the present emissions, EMEP/EEA, 2013) and in emission factors (up to 20%, EMEP/EEA, 2009). The future emissions depend on economic growth, penetration of new technologies and many other autonomic developments that are difficult to predict with certainty. These uncertainties in emissions will have less impact on the relative differences between scenarios than on each simulation; also, the differences between future scenarios will be less affected by uncertainties (since they share the same activity data) than the differences between present and future scenarios.

In general, the fixed boundary conditions in our simulations are expected to lead to an underestimation of the differences between scenarios. This effect will be larger for the longer lived species like H_2 and CO. Thus in reality, the effects of changing the emissions could be slightly larger, and they will depend on what happens in the rest of the world.

Because of the larger potential uncertainties in the individual simulations, we did not focus on comparisons with air quality limits. Instead, we focused on the relative differences between the different simulations, which are much less affected by model errors.

Like the previous studies regarding the possible future H_2 economy, our study does not account for the effects of future climate change on e.g. emissions, atmospheric chemistry or soil deposition. The possible effects of climate change on air quality are complex: for example, it is generally predicted that a warmer climate could lead to a slight increase in pollution levels, while an increase in precipitation can lead to pollution decrease (e.g. Colette et al., 2013; Fiore et al., 2012; Isaksen et al., 2009; Jacob and Winner, 2009). Model studies have shown that the climate impact on future air quality is in general much smaller than the impact of change in emissions. However, Hedegaard et al. (2013) found that in the Benelux area, climate change could have more influence on ground level ozone than the changes in ozone precursors, and would lead to an additional increase in O_3. In this case the increases in O_3 could be significantly larger than our estimates. Regarding our comparison between scenarios with and without H_2 cars, a warmer climate would affect all future simulations, and the resulting effect of climate on the relative differences between scenarios would likely be smaller than the absolute effect on each individual scenario.

In summary, we have shown that (1) air quality in Europe improves in the future, if we assume that current and planned legislation is successful; (2) air quality improves further with the introduction of H_2 vehicles, thus H_2 vehicles may be an effective pathway to fulfil the strict future EU air quality regulations; (3) with the decrease in traffic emissions, other emission categories become more important and will have to be better regulated; (4) the additional H_2 from leakages does not significantly affect the air quality in Europe, as long as the leak rate is kept below 4%.

Acknowledgments

This work was supported by the NWO-ACTS Sustainable Hydrogen (H_2) project 2007/00566/ACTS, grant numbers: 053.61.026 and 053.61.126.

M. E. Popa would like to thank A. Manders (TNO) for help with setting up the model. The authors would like to thank the two anonymous reviewers for their constructive comments.

Appendix A. Supplementary data

Supplementary data related to this article can be found at http://dx.doi.org/10.1016/j.atmosenv.2015.03.022.

References

Adamson, K.-A., Pearson, P., 2000. Hydrogen and methanol: a comparison of safety, economics, efficiencies and emissions. J. Power Sources 86, 548–555. http://dx.doi.org/10.1016/S0378-7753(99)00404-8.

Beelen, R., Raaschou-Nielsen, O., Stafoggia, M., Andersen, Z.J., Weinmayr, G., Hoffmann, B., Wolf, K., Samoli, E., Fischer, P., Nieuwenhuijsen, M., 2014. Effects of long-term exposure to air pollution on natural-cause mortality: an analysis of 22 European cohorts within the multicentre ESCAPE project. Lancet 383, 785–795. http://dx.doi.org/10.1016/S0140-6736(13)62158-3.

Bond, S.W., Alvarez, R., Vollmer, M.K., Steinbacher, M., Weilenmann, M., Reimann, S., 2010. Molecular hydrogen (H_2) emissions from gasoline and diesel vehicles. Sci. Total Environ. 408, 3596–3606. http://dx.doi.org/10.1016/j.scitotenv.2010.04.055.

Bond, S.W., Gül, T., Reimann, S., Buchmann, B., Wokaun, A., 2011. Emissions of anthropogenic hydrogen to the atmosphere during the potential transition to an increasingly H_2-intensive economy. Int. J. Hydrog. Energy 36, 1122–1135.

Colette, A., Bessagnet, B., Vautard, R., Szopa, S., Rao, S., Schucht, S., Klimont, Z., Menut, L., Clain, G., Meleux, F., 2013. European atmosphere in 2050, a regional air quality and climate perspective under CMIP5 scenarios. Atmos. Chem. Phys. 13, 7451–7471.

Colette, A., Granier, C., Hodnebrog, Ø., Jakobs, H., Maurizi, A., Nyiri, A., Bessagnet, B., D'Angiola, A., D'Isidoro, M., Gauss, M., 2011. Air quality trends in Europe over the past decade: a first multi-model assessment. Atmos. Chem. Phys. 11, 11657–11678.

Damen, K., van Troost, M., Faaij, A., Turkenburg, W., 2006. A comparison of electricity and hydrogen production systems with CO2 capture and storage. Part A: review and selection of promising conversion and capture technologies. Prog. Energy Combust. Sci. 32, 215–246. http://dx.doi.org/10.1016/j.pecs.2005.11.005.

DeMore, W.B., Sander, S.P., Golden, D.M., Hampson, R.F., Kurylo, M.J., Howard, C.J., Ravishankara, A.R., Kolb, C.E., Molina, M.J., 1994. Chemical Kinetics and Photochemical Data for Use in Stratospheric Modeling: Evaluation Number 11. Jet Propulsion Lab, Pasadena, CA (United States).

Derwent, R., Simmonds, P., O'Doherty, S., Manning, A., Collins, W., Stevenson, D., 2006. Global environmental impacts of the hydrogen economy. Int. J. Nucl. Hydrog. Prod. Appl. 1, 57–67.

EEA, 2010. Sectoral Shares of Tropospheric Ozone Precursors (Energy and Non-energy Components) in Total Emissions, EU-27. http://www.eea.europa.eu/data-and-maps/figures/sectoral-shares-of-tropospheric-ozone-precursors-energy-and-non-energy-components-in-total-emissions-eu.

EEA, 2013. Air Quality in Europe — 2013 Report. EEA. http://dx.doi.org/10.2800/92843.

EEA, 2014. European Union Emission Inventory Report 1990–2012 Under the UNECE Convention on Long-range Transboundary Air Pollution (LRTAP). Report No 12/2014.

EMEP/EEA, 2009. EMEP/EEA Air Pollutant Emission Inventory Guidebook — 2009. Technical report No 9/2009, Updated May 2012 (last accessed 13.03.14.). http://www.eea.europa.eu/publications/emep-eea-emission-inventory-guidebook-2009.

EMEP/EEA, 2013. EMEP/EEA Air Pollutant Emission Inventory Guidebook — 2013. Technical report No 12/2013 (last accessed 13.03.14.). http://www.eea.europa.eu/publications/emep-eea-guidebook-2013.

Erisman, J.W., Schaap, M., 2004. The need for ammonia abatement with respect to

secondary PM reductions in Europe. Environ. Pollut. 129, 159–163.
EU, 2008. Directive 2008/50/EC of the European Parliament and of the Council of 21 May 2008 on Ambient Air Quality and Cleaner Air for Europe. OJ L 152, 11.6.2008, pp. 1–44. http://eur-lex.europa.eu/LexUriServ/LexUriServ.do?uri=OJ:L:2008:152:0001:0044:EN:PDF.
Fiore, A.M., Naik, V., Spracklen, D.V., Steiner, A., Unger, N., Prather, M., Bergmann, D., Cameron-Smith, P.J., Cionni, I., Collins, W.J., 2012. Global air quality and climate. Chem. Soc. Rev. 41, 6663–6683.
Fountoukis, C., Nenes, A., 2007. ISORROPIA II: a computationally efficient thermodynamic equilibrium model for K^+–Ca^{2+}–Mg^{2+}–NH^{4+}–Na^+–SO_4^{2-}–NO_3^-–Cl^-–H_2O aerosols. Atmos. Chem. Phys. 7, 4639–4659. http://dx.doi.org/10.5194/acp-7-4639-2007.
GPWv2, 2000. Center for International Earth Science Information Network (CIESIN), Columbia University; International Food Policy Research Institute (IFPRI); World Resources Institute (WRI). Gridded Population of the World, Version 2 (GPWv2). Socioeconomic Data and Applications Center (SEDAC), Columbia University, Palisades, NY. http://sedac.ciesin.columbia.edu/gpw-v2/.
Hammer, S., Vogel, F., Kaul, M., Levin, I., 2009. The H2/CO ratio of emissions from combustion sources: comparison of top-down with bottom-up measurements in southwest Germany. Tellus B 61, 547–555.
Hedegaard, G.B., Christensen, J.H., Brandt, J., 2013. The relative importance of impacts from climate change vs. emissions change on air pollution levels in the 21st century. Atmos. Chem. Phys. 13, 3569–3585.
Hoek, G., Krishnan, R.M., Beelen, R., Peters, A., Ostro, B., Brunekreef, B., Kaufman, J.D., 2013. Long-term air pollution exposure and cardio-respiratory mortality: a review. Environ. Health 12, 43.
Houweling, S., Dentener, F., Lelieveld, J., 1998. The impact of nonmethane hydrocarbon compounds on tropospheric photochemistry. J. Geophys. Res. 103, 10673–10610, 10696.
Isaksen, I.S.A., Granier, C., Myhre, G., Berntsen, T.K., Dalsøren, S.B., Gauss, M., Klimont, Z., Benestad, R., Bousquet, P., Collins, W., 2009. Atmospheric composition change: climate–chemistry interactions. Atmos. Environ. 43, 5138–5192.
Jacob, D.J., Winner, D.A., 2009. Effect of climate change on air quality. Atmos. Environ. 43, 51–63.
Jacobson, M.Z., Colella, W.G., Golden, D.M., 2005. Cleaning the air and improving health with hydrogen fuel-cell vehicles. Science 308, 1901–1905.
Jacobson, M.Z., 2008. Effects of wind-powered hydrogen fuel cell vehicles on stratospheric ozone and global climate. Geophys. Res. Lett. 35.
Krol, M., Houweling, S., Bregman, B., Broek, M., Segers, A., Velthoven, P.V., Peters, W., Dentener, F., Bergamaschi, P., 2005. The two-way nested global chemistry-transport zoom model TM5: algorithm and applications. Atmos. Chem. Phys. 5, 417–432.
Kuenen, J.J.P., Visschedijk, A.J.H., Jozwicka, M., Denier van der Gon, H.A.C., 2014. TNO-MACC_II emission inventory: a multi-year (2003–2009) consistent high-resolution European emission inventory for air quality modelling. Atmos. Chem. Phys. Discuss. 14, 5837–5869. http://dx.doi.org/10.5194/acpd-14-5837-2014.
Kukkonen, J., Olsson, T., Schultz, D., Baklanov, A., Klein, T., Miranda, A., Monteiro, A., Hirtl, M., Tarvainen, V., Boy, M., Peuch, V.-H., Poupkou, A., Kioutsioukis, I., Finardi, S., Sofiev, M., Sokhi, R., Lehtinen, K.E.J., Karatzas, K., San José, R., Astitha, M., Kallos, G., Schaap, M., Reimer, E., Jakobs, H., Eben, K., 2012. A review of operational, regional-scale, chemical weather forecasting models in Europe. Atmos. Chem. Phys. 12, 1–87. http://dx.doi.org/10.5194/acp-12-1-2012.
Lovins, A.B., 2003. Letters: assessing the future hydrogen economy. Science 302, 226–229. http://dx.doi.org/10.1126/science.302.5643.226b.
Manders, A.M.M., Schaap, M., Hoogerbrugge, R., 2009. Testing the capability of the chemistry transport model LOTOS-EUROS to forecast PM10 levels in the Netherlands. Atmos. Environ. 43, 4050–4059.
Manders, A.M.M., Schaap, M., Querol, X., Albert, M.F.M.A., Vercauteren, J., Kuhlbusch, T.A.J., Hoogerbrugge, R., 2010. Sea salt concentrations across the European continent. Atmos. Environ. 44, 2434–2442.
Marécal, V., Peuch, V.-H., Andersson, C., Andersson, S., Arteta, J., Beekmann, M., Benedictow, A., Bergström, R., Bessagnet, B., Cansado, A., Chéroux, F., Colette, A., Coman, A., Curier, R.L., Denier van der Gon, H.A.C., Drouin, A., Elbern, H., Emili, E., Engelen, R.J., Eskes, H.J., Foret, G., Friese, E., Gauss, M., Giannaros, C., Guth, J., Joly, M., Jaumouillé, E., Josse, B., Kadygrov, N., Kaiser, J.W., Krajsek, K., Kuenen, J., Kumar, U., Liora, N., Lopez, E., Malherbe, L., Martinez, I., Melas, D., Meleux, F., Menut, L., Moinat, P., Morales, T., Parmentier, J., Piacentini, A., Plu, M., Poupkou, A., Queguiner, S., Robertson, L., Rouïl, L., Schaap, M., Segers, A., Sofiev, M., Thomas, M., Timmermans, R., Valdebenito, Á., van Velthoven, P., van Versendaal, R., Vira, J., Ung, A., 2015. A regional air quality forecasting system over Europe: the MACC-II daily ensemble production. Geosci. Model Dev. Discuss. 8, 2739–2806. http://dx.doi.org/10.5194/gmdd-8-2739-2015.
Mues, A., Kuenen, J., Hendriks, C., Manders, A., Segers, A., Scholz, Y., Hueglin, C., Builtjes, P., Schaap, M., 2014. Sensitivity of air pollution simulations with LOTOS-EUROS to the temporal distribution of anthropogenic emissions. Atmos. Chem. Phys. 14, 939–955.
Nakicenovic, N., Alcamo, J., Davis, G., De Vries, B., Fenhann, J., Gaffin, S., Gregory, K., Grübler, A., Jung, T.Y., Kram, T., 2000. In: Nakicenovic, Nebojsa, Swart, Robert (Eds.), Special Report on Emissions Scenarios, Working Group III, Intergovernmental Panel on Climate Change (IPCC). Cambridge University Press, Cambridge, ISBN 0521804930, p. 612.
Pieterse, G., Krol, M.C., Batenburg, A.M., Steele, L.P., Krummel, P.B., Langenfelds, R.L., Rockmann, T., 2011. Global modelling of H_2 mixing ratios and isotopic compositions with the TM5 model. Atmos. Chem. Phys. 11, 7001–7026. http://dx.doi.org/10.5194/acp-11-7001-2011.
Pieterse, G., Krol, M.C., Batenburg, A.M., Brenninkmeijer, C.A., Popa, M.E., O'Doherty, S., Grant, A., Steele, L.P., Krummel, P.B., Langenfelds, R.L., Wang, H.J., Vermeulen, A.T., Schmidt, M., Yver, C., Jordan, A., Engel, A., Fisher, R.E., Lowry, D., Nisbet, E.G., Reimann, S., Vollmer, M.K., Steinbacher, M., Hammer, S., Forster, G., Sturges, W.T., Rockmann, T., 2013. Reassessing the variability in atmospheric H_2 using the two-way nested TM5 model. J. Geophys. Res. Atmos. 118, 3764–3780. http://dx.doi.org/10.1002/Jgrd.50204.
Pope III, C.A., Burnett, R.T., Thun, M.J., Calle, E.E., Krewski, D., Ito, K., Thurston, G.D., 2002. Lung cancer, cardiopulmonary mortality, and long-term exposure to fine particulate air pollution. Jama 287, 1132–1141.
Prather, M.J., 2003. An environmental experiment with H_2? Science 302, 581–582. http://dx.doi.org/10.1126/science.1091060.
Sauter, F., van der Swaluw, E., Manders-Groot, A., Kruit, R.W., Segers, A., Eskes, H., 2012. LOTOS-Euros v1.8 Reference Guide.TNO-060-UT-2012–01451.
Schaap, M., Loon, M.V., Ten Brink, H.M., Dentener, F.J., Builtjes, P.J.H., 2004a. Secondary inorganic aerosol simulations for Europe with special attention to nitrate. Atmos. Chem. Phys. 4, 857–874.
Schaap, M., van der Gon, H.A.C., Dentener, F.J., Visschedijk, A.J.H., van Loon, M., ten Brink, H.M., Putaud, J.-P., Guillaume, B., Liousse, C., Builtjes, P.J.H., 2004b. Anthropogenic black carbon and fine aerosol distribution over Europe. J. Geophys. Res. Atmos. 109, 18207.
Schaap, M., Denier van der Gon, H.A.C., 2007. On the variability of black smoke and carbonaceous aerosols in The Netherlands. Atmos. Environ. 41, 5908–5920.
Schaap, M., Timmermans, R.M., Roemer, M., Boersen, G., Builtjes, P., Sauter, F., Velders, G., Beck, J., 2008. The LOTOS – EUROS model: description, validation and latest developments. Int. J. Environ. Pollut. 32, 270–290.
Schultz, M.G., Diehl, T., Brasseur, G.P., Zittel, W., 2003. Air pollution and climate-forcing impacts of a global hydrogen economy. Science 302, 624–627. http://dx.doi.org/10.1126/science.1089527.
Sillman, S., 1999. The relation between ozone, NOx and hydrocarbons in urban and polluted rural environments. Atmos. Environ. 33, 1821–1845.
Simpson, D., Fagerli, H., Jonson, J.E., Tsyro, S., Wind, P., Tuovinen, J.P., 2003. Transboundary Acidification, Eutrophication and Ground Level Ozone in Europe, Part I. Unified EMEP Model Description. EMEP Report 1/2003, EMEP, 74 pp.
Spath, P.L., Mann, M.K., 2000. Life Cycle Assessment of Hydrogen Production via Natural Gas Steam Reforming. National Renewable Energy Laboratory, Golden, CO.
Solazzo, E., Bianconi, R., Pirovano, G., Moran, M.D., Vautard, R., Hogrefe, C., Appel, K.W., Matthias, V., Grossi, P., Bessagnet, B., Brandt, J., Chemel, C., Christensen, J.H., Forkel, R., Francis, X.V., Hansen, A.B., McKeen, S., Nopmongcol, U., Prank, M., Sartelet, K.N., Segers, A., Silver, J.D., Yarwood, G., Werhahn, J., Zhang, J., Rao, S.T., Galmarini, S., 2013. Evaluating the capability of regional-scale air quality models to capture the vertical distribution of pollutants. Geosci. Model Dev. 6, 791–818. http://dx.doi.org/10.5194/gmd-6-791-2013.
Tromp, T.K., Shia, R.L., Allen, M., Eiler, J.M., Yung, Y.L., 2003. Potential environmental impact of a hydrogen economy on the stratosphere. Science 300, 1740.
Van Zanten, M.C., Sauter, F.J., Wichink Kruit, R.J., Van Jaarsveld, J.A., Van Pul, W.A.J., 2010. Description of the DEPAC Module: Dry Deposition Modelling with DEPAC_GCN2010. RIVM report 680180001/2010. RIVM, 74 pp.
Vautard, R., Moran, M.D., Solazzo, E., Gilliam, R.C., Matthias, V., Bianconi, R., Chemel, C., Ferreira, J., Geyer, B., Hansen, A.B., 2012. Evaluation of the meteorological forcing used for the air quality model evaluation international initiative (AQMEII) air quality simulations. Atmos. Environ. 53, 15–37. http://dx.doi.org/10.1016/j.atmosenv.2011.10.065.
Vautard, R., Van Loon, M., Schaap, M., Bergström, R., Bessagnet, B., Brandt, J., Builtjes, P.J.H., Christensen, J.H., Cuvelier, C., Graff, A., 2006. Is regional air quality model diversity representative of uncertainty for ozone simulation? Geophys. Res. Lett. 33 http://dx.doi.org/10.1029/2006GL027610.
Veziroglu, T.N., Barbir, F., 1992. Hydrogen–the wonder fuel. Int. J. Hydrog. Energy 17, 391–404. http://dx.doi.org/10.1016/0360-3199(92)90183-W.
Vogel, B., Feck, T., Grooß, J.-U., Riese, M., 2012. Impact of a possible future global hydrogen economy on Arctic stratospheric ozone loss. Energy Environ. Sci. 5, 6445–6452. http://dx.doi.org/10.1039/C2EE03181G.
Vollmer, M.K., Juergens, N., Steinbacher, M., Reimann, S., Weilenmann, M., Buchmann, B., 2007. Road vehicle emissions of molecular hydrogen (H_2) from a tunnel study. Atmos. Environ. 41, 8355–8369.
Wang, D., Jia, W., Olsen, S.C., Wuebbles, D.J., Dubey, M.K., Rockett, A.A., 2013a. Impact of a future H_2-based road transportation sector on the composition and chemistry of the atmosphere – part 1: tropospheric composition and air quality. Atmos. Chem. Phys. 13, 6117–6137. http://dx.doi.org/10.5194/acp-13-6117-2013.
Wang, D., Jia, W., Olsen, S.C., Wuebbles, D.J., Dubey, M.K., Rockett, A.A., 2013b. Impact of a future H_2-based road transportation sector on the composition and chemistry of the atmosphere – part 2: stratospheric ozone. Atmos. Chem. Phys. 13, 6139–6150. http://dx.doi.org/10.5194/acp-13-6139-2013.
Warwick, N.J., Bekki, S., Nisbet, E.G., Pyle, J.A., 2004. Impact of a hydrogen economy on the stratosphere and troposphere studied in a 2-D model. Geophys. Res. Lett. 31.
Whitten, G.Z., Hogo, H., Killus, J.P., 1980. The carbon-bond mechanism: a condensed kinetic mechanism for photochemical smog. Environ. Sci. Technol. 14, 690–700. http://dx.doi.org/10.1021/es60166a008.
WHO, 2002. The World Health Report 2002. World Health Organization, Geneva.
WHO, 2006. Air Quality Guidelines. Global Update 2005. Particulate Matter, Ozone, Nitrogen Dioxide and Sulfur Dioxide. World Health Organization, Regional

Office for Europe, Copenhagen, Denmark, ISBN 92 890 2192 6.
WHO, 2008. Health Risks of Ozone from Long-range Transboundary Air Pollution. World Health Organization, Regional Office for Europe, Copenhagen, Denmark.
WHO, 2013. Review of Evidence on Health Aspects of Air Pollution — REVIHAAP Project Technical Report. World Health Organization, Regional Office for Europe, Copenhagen, Denmark.
Yver, C., Schmidt, M., Bousquet, P., Zahorowski, W., Ramonet, M., 2009. Estimation of the molecular hydrogen soil uptake and traffic emissions at a suburban site near Paris through hydrogen, carbon monoxide, and radon-222 semicontinuous measurements. J. Geophys. Res. 114, D18304.
Yver, C., Schmidt, M., Bousquet, P., Ramonet, M., 2011. Measurements of molecular hydrogen and carbon monoxide on the Trainou tall tower. Tellus B 63, 52–63.
Zhang, L., Gong, S., Padro, J., Barrie, L., 2001. A size-segregated particle dry deposition scheme for an atmospheric aerosol module. Atmos. Environ. 35, 549–560.
Zittel, W., Altmann, M., 1996. Molecular hydrogen and water vapour emissions in a global hydrogen energy economy. In: Proceedings of the 11th World Hydrogen Energy Conference, Stuttgart, Germany, June 1996, pp. 71–82.